



AuNP-based biosensors for the diagnosis of pathogenic human coronaviruses: COVID-19 pandemic developments

Mohammad Ali Farzin¹ · Hassan Abdoos¹ · Reza Saber²

Received: 15 April 2022 / Revised: 17 June 2022 / Accepted: 21 June 2022 / Published online: 4 July 2022
© Springer-Verlag GmbH Germany, part of Springer Nature 2022

Abstract

The outbreak rate of human coronaviruses (CoVs) especially highly pathogenic CoVs is increasing alarmingly. Early detection of these viruses allows treatment interventions to be provided more quickly to people at higher risk, as well as helping to identify asymptomatic carriers and isolate them as quickly as possible, thus preventing the disease transmission chain. The current diagnostic methods such as RT-PCR are not ideal due to high cost, low accuracy, low speed, and probability of false results. Therefore, a reliable and accurate method for the detection of CoVs in biofluids can become a front-line tool in order to deal with the spread of these deadly viruses. Currently, the nanomaterial-based sensing devices for detection of human coronaviruses from laboratory diagnosis to point-of-care (PoC) diagnosis are progressing rapidly. Gold nanoparticles (AuNPs) have revolutionized the field of biosensors because of the outstanding optical and electrochemical properties. In this review paper, a detailed overview of AuNP-based biosensing strategies with the varied transducers (electrochemical, optical, etc.) and also different biomarkers (protein antigens and nucleic acids) was presented for the detection of human coronaviruses including SARS-CoV-2, SARS-CoV-1, and MERS-CoV and lowly pathogenic CoVs. The present review highlights the newest trends in the SARS-CoV-2 nanobiosensors from the beginning of the COVID-19 epidemic until 2022. We hope that the presented examples in this review paper convince readers that AuNPs are a suitable platform for the designing of biosensors.

Keywords AuNPs · CRISPR · Human coronaviruses · Nanobiosensors · Pathogenic

Introduction

RNA-positive viruses are more dangerous than DNA viruses, due to their much higher mutation rate [1]. In addition, many RNA viruses can cause persistent infections in the host body, occasionally causing a chronic illness or reactivation [2]. One of these RNA viruses that plagues the world is the new human coronavirus (CoV) called SARS-CoV-2.

Two years after the outbreak of COVID-19 caused by SARS-CoV-2, this pandemic does not appear to be over. The new species of Omicron is still spreading around the world despite approved vaccines. This suggests that scientists need

to find new ways to fight the new coronavirus. It seems that the carrier screening and diagnosing infection in asymptomatic infected people along with high vaccination coverage can help fight this pandemic.

At present, due to the rapid growth and high demand for the testing of suspected and asymptomatic patients, as well as the emergence of mutant strains, finding the point-of-care (PoC) diagnostic methods with high accuracy and sensitivity is a main challenge. Although RT-PCR is a gold standard for the COVID-19 diagnosis, it requires a sufficient amount of virus RNA in the patient sample [3, 4]. Since the concentration of viral RNA in the early stages of the disease is very low, this can affect the results obtained [5]. Also, factors such as sample type, sampling time, sample quality in terms of cellular materials, and how the sample is sent and stored in the laboratory can strongly affect the RNA concentration and sometimes lead to false-negative results [4]. In addition, nucleic acid testing for the RNA-positive viruses involves additional steps of reverse translation of RNA to DNA before amplification. Therefore, RT-PCR is time-consuming and costly and is not suitable for use in

✉ Hassan Abdoos
h.abdoos@semnan.ac.ir

¹ Department of Nanotechnology, Faculty of New Sciences and Technologies, Semnan University, P. O. Box: 35131-19111, Semnan, Iran

² Department of Medical Nanotechnology, School of Advanced Technologies in Medicine, Tehran University of Medical Sciences, Tehran, Iran

PoC diagnostics [6]. On the other hand, the ability of RT-PCR to amplify small amounts of the target DNA pattern in order to increase sensitivity allows the amplification of small amounts of contaminations arising from poor and non-specific probes, laboratory, reagents, and samples [4]. Although, the most important source of contamination is the presence of amplified molecules from the previous PCR. These unexpected contaminations lead to false-positive achievements [4, 5].

Biosensors are a promising alternative for RT-PCR-based virus detection. These powerful tools are able to detect ultratrace levels of CoV RNA strands in the early stages of the disease without nucleic acid amplification and reverse transcription. They are a combination of different advanced technologies such as electronic, photonic, nanotechnology, and biotechnology. The use of emerging advanced technologies, such as microchips, smartphones, wireless systems, clustered regularly interspaced short palindromic repeats (CRISPR), and nanomaterials, can lead to the design of new generation biosensors for the PoC diagnosis of diseases. Among nanomaterials, the gold nanoparticles (AuNPs) have found special applications in the construction of biosensors due to their outstanding electrochemical and optical characteristics. In addition, the strong affinity of AuNPs for the thiol-containing biomolecules makes them suitable platforms for the immobilization of biological receptors [7, 8].

It is well known that the resonant oscillation of conduction electrons is more prominent in metal nanoparticles, due to the very high surface-to-volume ratio (especially in dimensions such as below 20 nm). A phenomenon called surface plasmonic resonance (SPR) is observed at certain frequencies. These frequencies are within the visible light frequency range for noble metal NPs such as AuNPs and AgNPs, which makes this phenomenon doubly attractive. AuNPs indicate an SPR band of ~520 nm in the visible region [9]. With increasing the size of AuNPs, the frequency of surface plasmonic resonance decreases (known as red-shifting), and as a result, waves with lower frequency are absorbed. So, the color seen will have waves with a higher frequency. This explains the change in color of AuNPs from red to blue as they get larger. The ability to change the color of AuNPs from red to blue due to their aggregation is the basis of the design of many colorimetric biosensors. In addition to size, the optical features of AuNPs are strongly influenced by their shape. With the change of AuNPs shape from sphere to rod, the SPR band splits into two peaks of ~540 and 700 nm. This ability to change the SPR wavelength from the visible to NIR makes AuNPs very unique for use in biological sensors [10].

AuNPs as the outstanding fluorescence quenchers are 9 to 10 times more efficient than ordinary small molecular quenchers [11]. This phenomenon has attracted much attention both in basic studies and in practical applications. Up

to now, a large number of on/off fluorescence biosensors include quantum dots (QDs) and AuNPs have been designed [12–14].

The electrochemical properties of AuNPs have led to their widespread applications as electrode modifiers. The presence of AuNPs on the electrode surface plays a critical role in the electron transfer acceleration [15–18]. These nano-platforms increase electrochemically active surface area [16, 17]. In addition, several studies reported the electrocatalytic activities of AuNPs in the electrochemical reactions [19–22].

In this review, we discuss the ongoing developments in the AuNP-based biosensing strategies for the early detection of human coronaviruses including highly pathogenic (SARS-CoV-2, SARS-CoV-1, and MERS-CoV) and lowly pathogenic (HCoV-NL63, HCoV-HKU1, HCoV-OC43, and HCoV-229E). We try to give a comprehensive view of the role of these nanoparticles in the designing of biosensors. Unlike the recently published review articles [23–29] that covered the performed studies on the SARS-CoV-2 diagnosis in 2020–2021, this manuscript focuses on the newest trends for the sensing of all human coronaviruses using the AuNPs from the beginning of the COVID-19 epidemic until 2022. This paper includes a detailed overview of biosensing strategies using the varied transducers (electrochemical, optical, etc.) and also different biomarkers (protein antigens and nucleic acids) with a special emphasis on gold nanomaterials. We believe that this novel summary will help the researchers design and validate efficient sensing strategies for commercial applications.

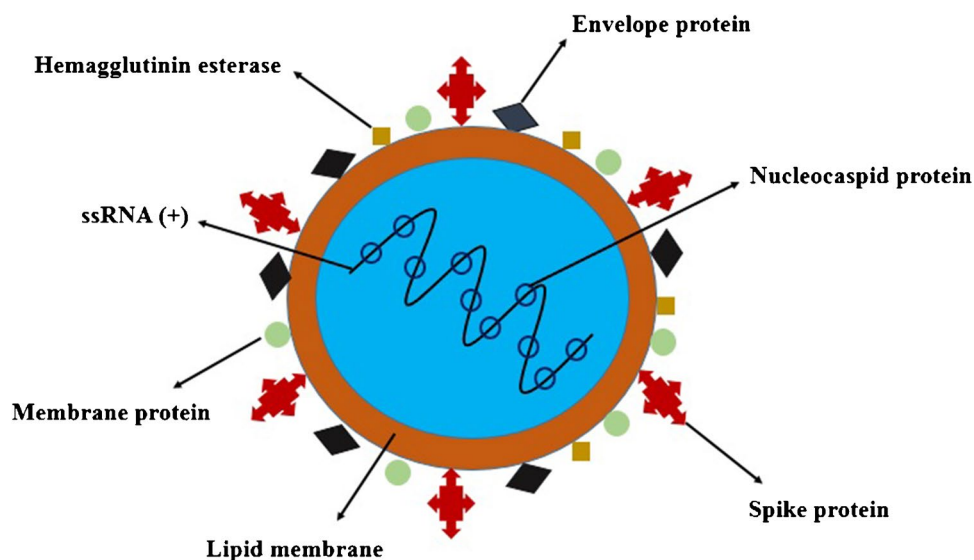
AuNP-based sensing methods for detection of coronaviruses

The biosensing devices are a hot topic in the diagnosis of biomarkers, which vary according to detection transducers such as electrochemical, optical, etc. and also the used biomarkers.

There are two main types of COVID-19 biomarkers: protein antigens and nucleic acids (Fig. 1). The antigen test determines viral proteins, such as nucleocapsid (N), envelope (E), and spike (S) proteins. These proteins are among the most valuable biomarkers of antigens for COVID-19 assessment [30]. The E protein, along with the membrane (M) protein and S protein, is embedded in a lipidic membrane to form the viral outer wall.

Many molecular diagnostic tests have used RT-PCR technology to target various genomic regions of SARS-CoV-2. The five genomic regions of the SARS-CoV-2 including N, E, S, RNA-dependent RNA polymerase (RdRP), and open reading frame (ORF1ab) genes have been selected for the designing of assays [31, 32].

Fig. 1 The structure of SARS-CoV-2



SARS-CoV-1 or SARS-CoV is ~79.5% genetically similar to the SARS-CoV-2 [33, 34]. The symptoms associated with this infection are very similar to those of COVID-19 [34]. However, the transmission of SARS-CoV-1 is lower than SARS-CoV-2 in the first 5 days of infection [35].

MERS-CoV is another fatal human coronavirus with the largest genomic size (~30.11 kb) [36]. As mentioned, SARS-CoV-2 has ~79.5% genomic similarity to SARS-CoV-1 while only about 50% similar to MERS-CoV [36]. MERS-CoV has the same structure proteins as two previously known groups of coronaviruses. However, the fatality rate of MERS-CoV infection is about 35%, which is higher than the SARS-CoV-1 (around 11%) [37].

The focus of this review will be the AuNP-based sensing platforms for the determination of the main biomarkers of these viruses, such as protein antigens and nucleic acids that can be analyzed using electrochemical, optical, and other detection methods.

Electrochemical sensing methods

Since the introduction of the first enzyme electrode to measure glucose by Prof. Clark, electrochemical biosensors have been growing rapidly. Today, the electrochemical biosensors are widely used in various fields, especially medicine. Meanwhile, research in this area remains strong and efforts to commercialize new ideas continue.

Electrochemical biosensors are well known for their numerous advantages such as ultratrace detection limits, simplicity, wide accessibility, low cost, low sample volume, high selectivity, and high sensitivity [38, 39]. More importantly, these powerful tools can be miniaturized to portable microchips due to the developments in the affordable

production of microelectronic circuits and processing systems [39].

This section focuses on state of the art of coronavirus detection by utilizing AuNP-based electrochemical biosensing platforms. For example, Layqah and Eissa [40] developed an electrochemical immunosensor for the determination of MERS-CoV S protein using an AuNP-modified carbon electrode array. The measurement was based on indirect competition between the immobilized MERS-CoV S protein for a constant concentration of antibody and free virus. Electrochemical measurements using $[\text{Fe}(\text{CN})_6]^{3-/4-}$ redox couple were recorded using voltammetry. A good linear relationship between the electrode responses and target concentrations was observed from 0.001 to 100 ng mL⁻¹. This assay with a LOD of 1.0 pg mL⁻¹ was performed in 20 min.

To better understand the efficiency of AuNPs in detecting COVID-19, the latest advances in the electrochemical SARS-CoV-2 biosensors are presented in Table 1 [41–59].

Colorimetric sensing methods

Colorimetric sensors are a class of optical sensors that change their color when influenced by external stimuli. These sensors are very popular and widespread, especially because of their simplicity and availability [38, 61]. Especially, the naked-eye colorimetric biosensors are the most suitable devices for the point-of-care diagnosis due to the production of visible signals without the need for an excitation light source or complex equipment.

The colorimetric detection of SARS-CoV-2 assisting AuNPs has been widely studied because of the strong SPR absorption band of AuNPs in the visible region. The color changes as a result of aggregation of AuNPs can be led to

Table 1 Summary of previously reported papers for the electrochemical determination of SARS-CoV-2 using AuNPs

Detection mode	Format of modified electrode	LOD	DLR	Ref
Amperometry	FTO/AuNPs/Ab/S protein	10 fM (in buffer) 120 fM (in spiked saliva samples)	1 fM–1 μ M	[41]
Potentiometry	Filter paper/AuNPs/graphene/ssDNA/N gene	6.9 copies μ L ⁻¹	5.854–585.4 $\times 10^7$ copies μ L ⁻¹	[42]
SWV	SPGE/AuNPs/Ab/S protein	1 pg mL ⁻¹	1 pg mL ⁻¹ –10 ng mL ⁻¹	[43]
SWV	PDMS/Au microcuboid/Ab/S protein	276 fM	5 pM–100 nM	[44]
DPV	GCE/Bi ₂ WO ₆ /Bi ₂ S ₃ composite/Ab/N protein/Ab/g-C ₃ N ₄ /AuNPs/WO ₃ composite	3.00 fg mL ⁻¹	0.01–1 pg mL ⁻¹	[45]
DPV	FTO/AuNPs/Ab/S protein	0.63 fM (in buffer) 120 fM (in spiked saliva samples)	1 fM–1 μ M	[46]
DPV	RGO/AuNSs/Ab/S protein	0.001 fg mL ⁻¹	–	[47]
EIS	SPGE/MIP/SARS-CoV-2-RBD	0.7 pg mL ⁻¹	2.0–40.0 pg mL ⁻¹	[48]
EIS	GIE/APTES/diamond nanopowder-CDI/N-specific aptamer/N protein	0.389 fM	1 fM–100 pM	[49]
DPV	GE/dual aptamer/N48 and N61 proteins/GQH DNzyme/dual aptamer/HRP/Au@Pt NPs-MOF MIL53(AI)	8.33 pg mL ⁻¹	0.025–50 ng mL ⁻¹	[50]
DPV	SPE/Au@Fe ₃ O ₄ -CP-HT/ORF1ab/SCX8-RGO-Au-TB-LP-AP (smartphone)	3 aM or 200 copies mL ⁻¹	10 ⁻¹⁷ –10 ⁻¹² M	[51]
Electric resistance (conductivity)	AuNPs linked to organic ligands/VOCs	–	–	[52]
–	Ti/AuNPs/cDNA/SARS-CoV-2 RNA	–	–	[53]
EIS	3D-printed G/PLA/AuNPs/Ab/S protein	0.5 μ g mL ⁻¹	1–10 μ g mL ⁻¹	[54]
DPV	SPCE/NC (MoS ₂ NSs, GNPs, CHT)/AuNFs/SA/Biotin-crRNA-MB/Cas13a protein/ORF and S gene	4.4 $\times 10^{-2}$ fg mL ⁻¹ (ORF) 8.1 $\times 10^{-2}$ fg mL ⁻¹ (S gene)	1 $\times 10^{-1}$ –1 $\times 10^5$ fg mL ⁻¹	[55]
EIS	SPCE/SiO ₂ @Zr6carboxylate MOF (UiO-66)/Ab/S protein	100.0 fg mL ⁻¹	100.0 fg mL ⁻¹ –10.0 ng mL ⁻¹	[56]
EIS	SPCE/AuNPs/MAA/Ab/S protein	3.16 pM (83.7 pg mL ⁻¹)	10 ⁻¹¹ –10 ⁻⁷ mol L ⁻¹	[57]
EIS	ITO/PPy/AuNP/cystamine/cDNA/N gene	258.01 copies μ L ⁻¹	800–4000 copies μ L ⁻¹	[58]
DPV	SPCE/magnetic beads/ACE2/S protein/ACE2-AuNPs	0.35 ag mL ⁻¹	–	[59]
DPV	Paper electrode/GNC/Au@CD NPs/cDNA/RdRP gene	0.15 pM	0.5 pM–12.00 nM	[60]

LOD limit of detection, *DLR* dynamic linear range, *FTO* fluorine-doped tin oxide electrode, *AuNPs* gold nanoparticles, *Ab* antibody, *S* spike, *N* nucleocapsid, *SWV* square wave voltammetry, *SPGE* screen-printed gold electrode, *PDMS* polydimethylsiloxane, *GCE* glassy carbon electrode, *Bi₂WO₆/Bi₂S₃* bismuth tungstate/bismuth sulfide composite, *g-C₃N₄/AuNPs/WO₃* graphitic carbon nitride sheet decorated with AuNPs and tungsten trioxide sphere composite, *DPV* differential potential voltammetry, *RGO* reduced graphene oxide, *AuNSs* gold nanostars, *MIP* molecular-imprinted polymer, *EIS* electrochemical impedance spectroscopy, *GIE* gold-interdigitated electrode, *APTES* (3-aminopropyl) triethoxysilane, *CDI* 1,1'-carbonyldiimidazole, *GE* gold electrode, *HRP* horseradish peroxidase, *GQH* hemin/G-quadruplex, *SPCE* screen-printed carbon electrode, *SCX8-RGO* p-sulfocalix[8]arene-functionalized reduced graphene oxide, *TB* toluidine blue, *L strand* label strand, *A strand* auxiliary strand, *C strand* capture strand, *ORF1ab* open reading frame genes, *VOCs* volatile organic compounds, *G/PLA* graphene/poly(lactic acid), *NC* nonocomposite, *MoS₂NSs* MoS₂ nanosheets, *GNPs* graphene nanoplates, *CHT* chitosan, *AuNFs* gold nanoflowers, *SA* streptavidin, *crRNA* complementary reporter RNA, *MB* methylene blue, *MOF* metal–organic framework, *MAA* mercaptoacetic acid, *ITO* indium tin oxide, *PPy* polypyrrole, *ACE2* angiotensin-converting enzyme 2 peptide, *GNC* graphite nanocrystal, *CD* carbon dot.

the naked-eye detection of COVID-19. For example, Rodríguez-Díaz et al. [62] designed the colorimetric genosensors using the molecular beacon–functionalized AuNPs for the detection of RdRP, E, and S genes. To reach this goal, both the AuNP and cholesterol molecules were attached to the two ends of the molecular beacon. An increase in the target gene led to the molecular beacon opening and hybridization to the target gene, resulting in the cholesterol exposure to

the solution. The cholesterol molecules caused AuNPs to aggregate. As the size of the AuNPs increased, their color changed to blue, which was visible to the naked eye. One of the advantages of these genosensors is their stability for several months without a significant reduction in their activity. In addition, these sensors allow the SARS-CoV-2 sequence to be detected by the naked eye in 15 min. Kumar and co-workers [63] developed a colorimetric RdRP genosensor

based on the aggregation-induced color change of AuNPs in the nasopharyngeal samples of COVID-19 patients. As seen in Fig. 2, a mixture of cDNA strands, SARS-CoV-2 RdRP genes, and salt was denatured at 95 °C for 30 s and then annealed at 60 °C for 60 s. With the addition of pink-color AuNPs to the mixture, they were aggregated at 10 min and the color of nanoparticles changed to blue. However, the color of AuNPs retained pink in the presence of RNA samples from COVID-19-negative volunteers. The proposed sensing strategy was able to determine SARS-CoV-2 genes up to 0.5 ng in less than 30 min.

In another research, the colorimetric assessment of S protein of SARS-CoV-2 with AuNP-based immunosensors was suggested by Karakus et al. [43]. In the presence of the target antigen, the antibody-functionalized AuNPs were aggregated as a result of antibody–antigen interaction (Fig. 3). As seen, the color of the aggregated nanoparticles turned from red to purple. This change in color was detected using the naked eye or UV–Vis spectroscopy. This high-specific sensing assay showed a LOD of 48 ng mL⁻¹. Another step-by-step strategy was designed by Alafeef et al. [64] for colorimetric detection of the N gene. The plasmonic oligo probe–attached AuNPs were used to detect the amplified genes of SARS-CoV-2. The specific binding of oligo probes to their target sequences led to the aggregation of plasmonic AuNPs. Determination was performed with the observation

of color change by the naked eye with a limit of detection (LOD) of 10 copies μL^{-1} .

Pramanik and co-workers [65] presented the development of antibody-functionalized AuNPs for the colorimetric determination of SARS-CoV-2 S protein. In the presence of the target protein, the antibody-functionalized AuNPs were aggregated due to the antigen–antibody interaction. Therefore, the surface plasmon coupling between antibody-functionalized AuNPs resulted in a color change from pink to blue. This naked-eye sensing strategy was able to determine S antigen within 5 min with a LOD of 1 ng mL⁻¹. Ventura et al. [66] introduced a colorimetric biosensor based on the antibody-attached AuNPs for the quantification of S, E, and M proteins in the nasal and throat swabs using the UV–Vis spectrophotometer. In the presence of target proteins, an extinction spectrum of antibody-attached AuNPs was redshifted in a few minutes. The authors claimed that the presented method was able to measure low viral load with a detection limit close to that of RT-PCR. Moitra and co-workers [67] developed a visual assay based on the DNA probe–functionalized AuNPs for the assessment of the N gene within 10 min. In the presence of SARS-CoV-2 genes, the oligo probe–functionalized AuNPs were agglomerated, leading to a change in its surface plasmon resonance. When the ribonuclease H (RNaseH) was added to the RNA–DNA duplex, it cleaved the RNA strands, resulting in a visually

Fig. 2 Schematic representation of the visual sensing assay of SARS-CoV-2 RNA target [63]

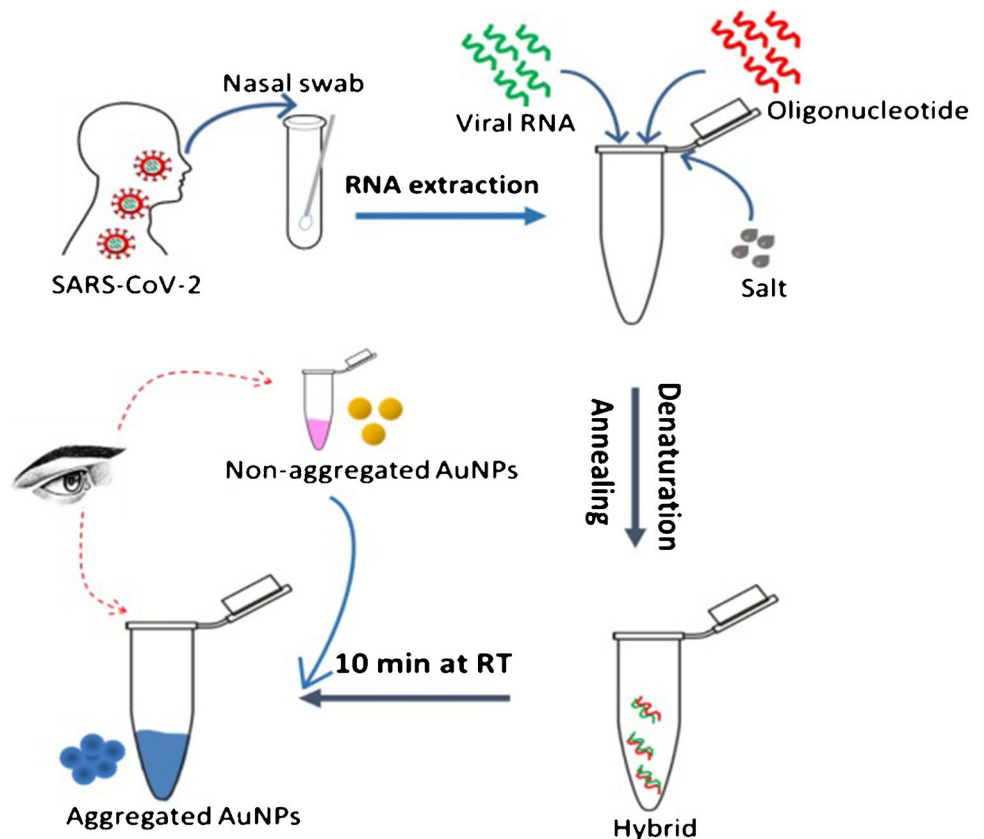
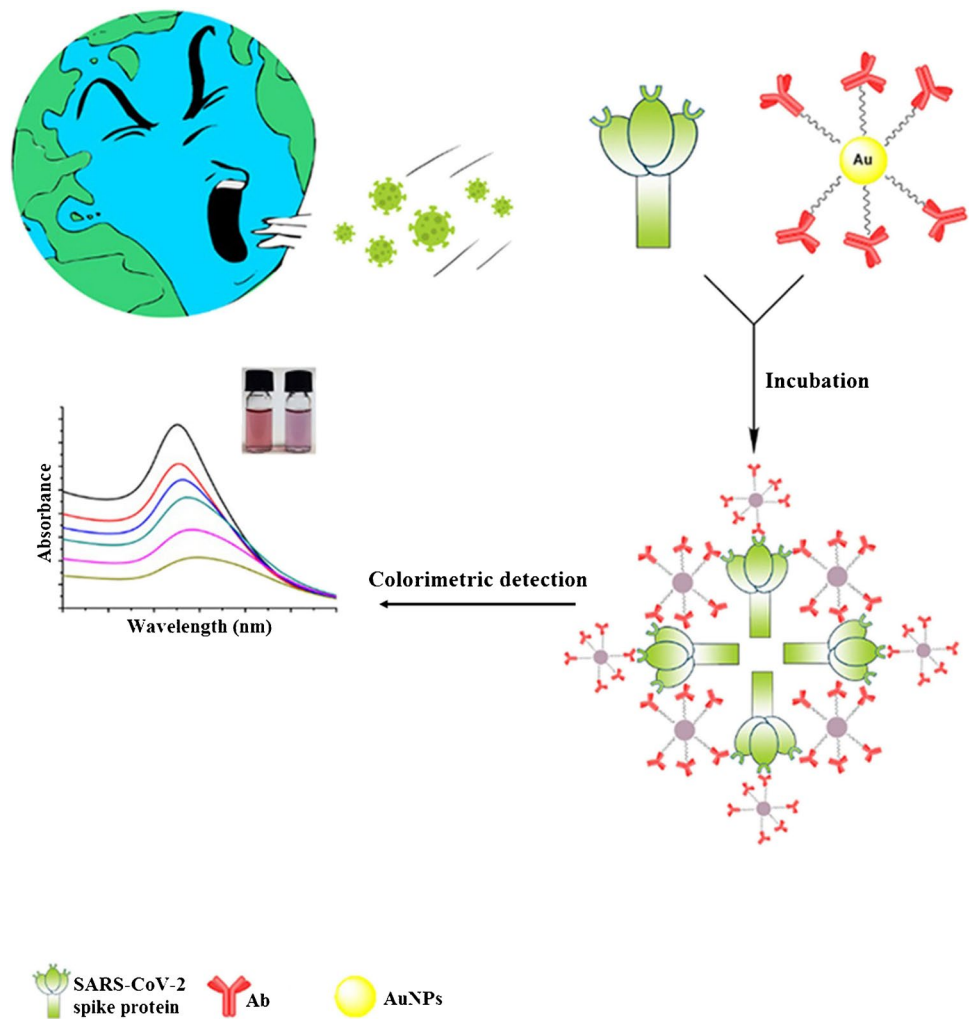


Fig. 3 UV–Vis sensing assay of SARS-CoV-2 S protein based on the aggregation of AuNPs-mAb in the presence of target protein [43]; reprinted by permission from Elsevier Publisher



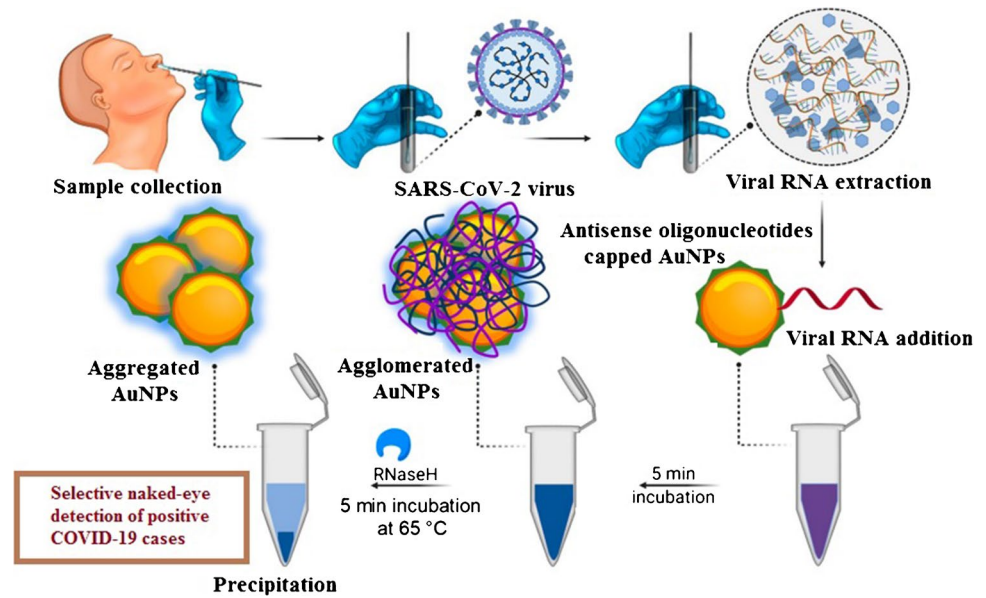
detectable precipitate from the solution due to the additional agglomeration among the AuNPs (Fig. 4). The analytical performance of this sensing protocol was evaluated by calculating the LOD which was $0.18 \text{ ng } \mu\text{L}^{-1}$.

Aithal et al. [68] used aptamers as the specific bioreceptors for early diagnosis of COVID-19. Aptamers are ssDNA or ssRNA strands that bind to their targets by folding into a 3D conformation with affinity binding comparable to antibodies [68, 69]. These bioreceptors are more stable and less expensive than antibodies. This research group described a test using the anti-S aptamer-functionalized AuNPs to determine this protein. The addition of MgCl_2 salt (salt M), as a coagulant, to the target-free solution led to the increased agglomeration of functionalized AuNPs and redshifted absorbance (Fig. 5A). The salt M with the surface charges of the aptamer-functionalized AuNPs formed complexes and decreased the net charge of aptamer-functionalized AuNPs, which promoted agglomeration. With the target addition, the aptamers on the surfaces of AuNPs bound specifically with the S protein and increased the electrostatic charge, leading

to an enhanced steric stabilization and decreased agglomeration (Fig. 5B). The UV–Vis spectra with and without agglomeration are schematically illustrated in Fig. 5C. This colorimetric strategy can detect up to 16 nM of S protein in the buffer solution. In another attempt, Behrouzi and Lin [70] described the aggregation of antibody-functionalized AuNPs for the detection of SARS-CoV-2 N proteins. This strategy produced observable results by the naked eye in 5 min with a LOD of 150 ng mL^{-1} .

The CRISPR/Cas systems including a guide RNA (gRNA) and a Cas12a protein are widely utilized to improve the sensitivity and specificity of molecular assays [71]. They make the determination of nucleic acids possible with a single molecular sensitivity [72]. So, the CRISPR/Cas systems can play an important role in the global fight against the COVID-19 pandemic using the SARS-CoV-2 detection [73]. The gRNA directs Cas protein to cleave specific sequences of RNA or DNA molecules [74]. These systems specifically identify the amplicons that are amplification products and improve the determination specificity. In fact, the specific

Fig. 4 Schematic representation for the visual detection of SARS-CoV-2 RNA using the oligo probe-attached AuNPs [67]; reprinted by permission from ACS Publisher



sequences of complementary amplicons of gRNA sequences can only activate the CRISPR/Cas systems. Using these systems, Cao and co-workers [75] described a colorimetric sensing strategy for the isothermal and visual detection of N and E genes. They integrated the reverse transcription loop-mediated isothermal amplification (RT-LAMP) and the cleavage activity of CRISPR/Cas12a to facilitate sequence-dependent aggregation of AuNPs. As seen in Fig. 6, the Cas12a-gRNA specifically bound to the target sequence of the amplicon and cleaved the DNA loop of the hairpin transducer. As a result, the hairpin was destabilized and the RNA cross-linker was released from its hybrid. Then, the

released RNA cross-linker was hybridized with the ssDNA on AuNPs, leading to the aggregation of AuNPs and the change of color from red to purple. Based on this sensing strategy, the authors claimed that the N and E genes of SARS-CoV-2 could be detected visually in 45 min. Ma et al. [76] developed a smartphone-based genosensor using the CRISPR/Cas12a system for visual detection of the SARS-CoV-2 N gene. The N gene target caused degradation of linker ssDNA using the CRISPR/Cas12a system to bind two AuNPs, resulting in the disaggregation of AuNPs and thus the change of color from blue to red. This change of color was detected by the naked eye as well as a smartphone with

Fig. 5 Schematic illustration for determination of SARS-CoV-2 spike protein using AuNPs functionalized with aptamers. **A** The addition of MgCl₂ salt (salt M), as a coagulant, to the target-free solution led to the increased agglomeration of functionalized AuNPs and redshifted absorbance. **B** With the target addition, the aptamers on the surfaces of AuNPs bound specifically with the spike protein and increased the electrostatic charge, leading to an enhanced steric stabilization and decreased agglomeration. **C** Schematic illustration of UV-Vis spectra with and without agglomeration [68]; reprinted by permission from Elsevier Publisher

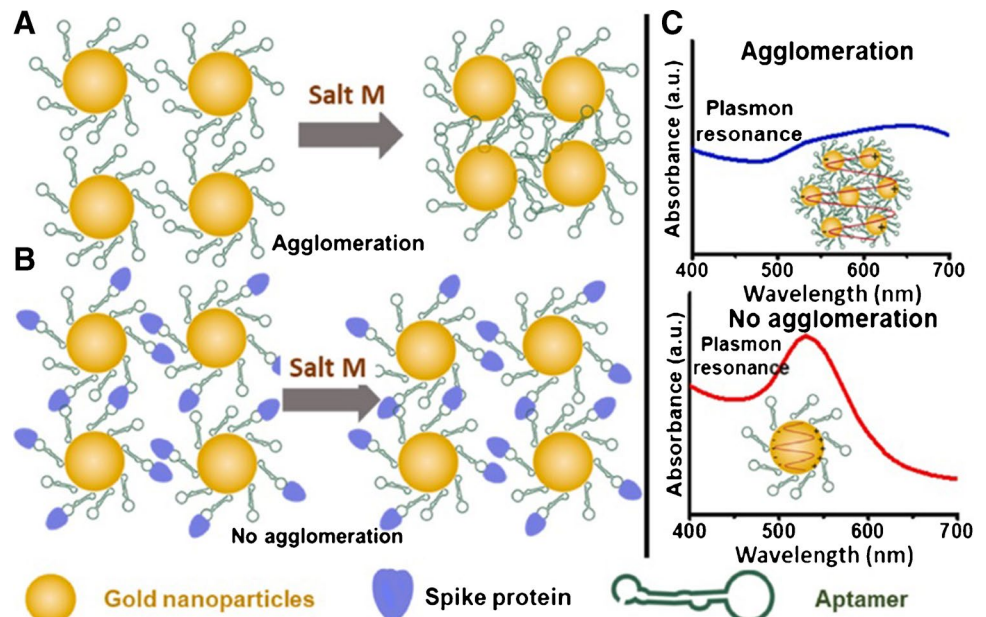
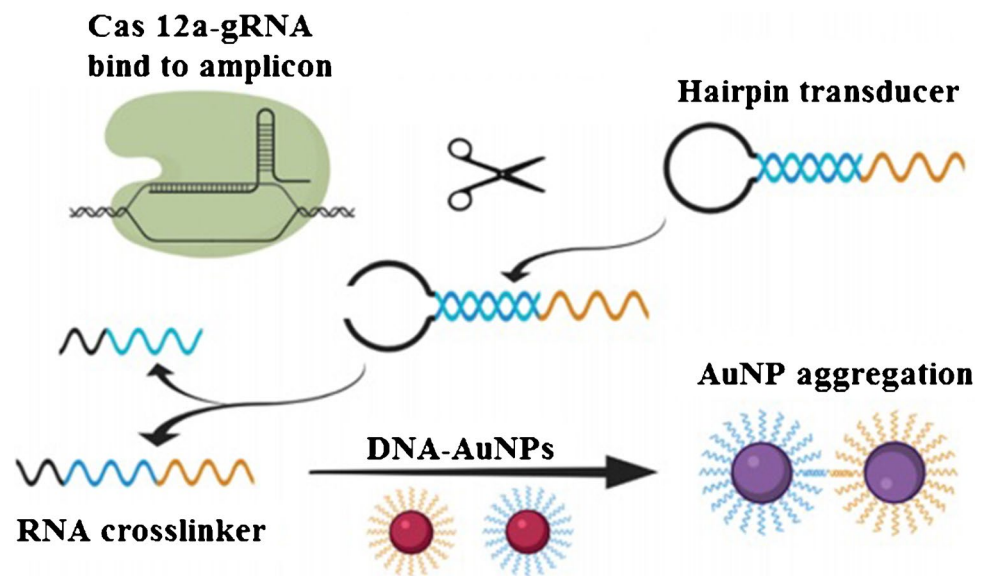


Fig. 6 The principle of Cas12a-mediated AuNP aggregation [75]; reprinted by permission from RSC Publisher



a Color Picker App. The designed genosensor indicated single-copy resolution as confirmed by LOD of $1 \text{ copy } \mu\text{L}^{-1}$ with no cross-reactivity. In another attempt, Jiang and co-workers [77] presented a magnetic visual genosensor using the CRISPR/Cas12a for SARS-CoV-2 RNA determination. In this strategy, the extracted RNA strands of SARS-CoV-2 were detected by the naked eye based on the AuNP probes with a LOD of 50 RNA copies per reaction.

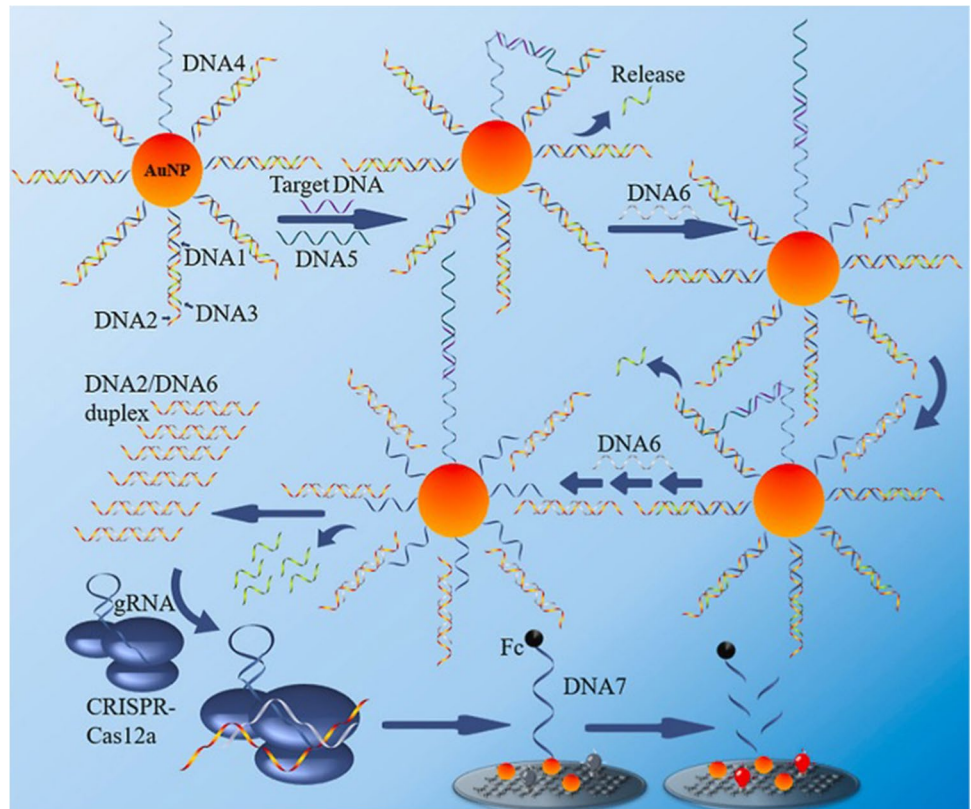
ECL-based sensing methods

Electrochemiluminescence (ECL) strategy can be regarded as a combination of both spectrometric and electrochemical assays, thus holding the advantages of both two methods. The high sensitivity for the determination of analytes with very small values and also in a short time are the advantages of this method. However, ECL suffers from several limitations such as a complex interface that enhances the non-specific adsorption, simple diffusion of luminescent reagents in homogeneous solutions, inability for the reversible modulation and poor long-term stability of luminescent materials, etc. [74, 78]. Using the combination of 3D-DNA Walker and CRISPR/Cas12a system, Zhang and co-workers [79] reported an MXene (2D materials made up of surface-modified carbide)-based genosensor for the ECL determination of SARS-CoV-2 RdRP gene. In this strategy, the amplification of RdRP gene into a segment of dsDNA using a 3D DNA walker led to the activation of cleavage activity of CRISPR/Cas12a. Then, an MXene-based ECL material was designed using the polyethylenimine (PEI)-Ru@Ti₃C₂@AuNPs for the construction of an ECL biosensor. The activated CRISPR/Cas12a cleaved the ssDNA on the genosensor surface and turned away the ferrocene attached

to the end of DNA from the electrode surface. This led to the increasing ECL signal (Fig. 7). The extent of the change in ECL reflects the concentration of the RdRP gene. Using this system, the SARS-CoV-2 RdRP gene was determined with a LOD of 12.8 aM.

Yao et al. [80] also reported an MXene Ti₃C₂ for the fabrication of an ECL RdRP genosensor (Fig. 8). They designed a sensing strategy using the Au@Ti₃C₂@PEI-Ru(dcbpy)₃²⁺ nanocomposites with excellent ECL performance for COVID-19 diagnosis. The MXene-Ti₃C₂ had good electrical conductivity and a large specific surface area that dispersed AuNPs uniformly and loaded the high concentrations of Ru(dcbpy)₃²⁺. Using the Nb.BbvCI, as a nicking endonuclease that cleaves only one strand of DNA on a dsDNA, large numbers of hairpin DNAs were removed by the amplification strategy of the DNA walker. In this strategy, the DNA-templated silver nanoclusters (DNA@AgNCs) were utilized to quench the ECL signal. This ECL genosensor could determine the SARS-CoV-2 RdRP gene in a linear range of 1 fM to 100 pM and a LOD of 0.21 fM. In another attempt, a three-stranded Y-type DNA-induced hybridization chain reaction (HCR) was designed for the ECL detection of the SARS-CoV-2 RdRP gene by Zhang et al. [81]. Y-DNA prepared by hybridizing three ssDNA (Y1, Y2, and Y3) provided a nucleic acid scaffold for the amplification reaction on the surface of AuNPs-g-C₃N₄-modified electrode. Using this biosensor, the SARS-CoV-2 RdRP was determined based on the resonance energy transfer (RET)-ECL strategy between Au-g-C₃N₄ and Ru. A LOD of 59 aM was achieved in the pharyngeal swabs. Gutiérrez-Gálvez and co-workers [82] introduced a combination of gold nanomaterials (AuNMs) and carbon dots (CDs) for the designing of ECL SARS-CoV-2 genosensor. In this study, a mixture of AuNMs with

Fig. 7 Schematic representation of the ECL biosensor based on 3D-DNA walker and CRISPR/Cas 12a for the SARS-COV-2 RdRP detection [79]; reprinted by permission from Elsevier Publisher



different shapes (AuNPs and gold triangles (AuNTs)) was utilized as a platform for the ECL detection of the ORF1ab

fragment of SARS-CoV-2 RNA. The described genosensor showed an acceptable recovery in the spiked human serum

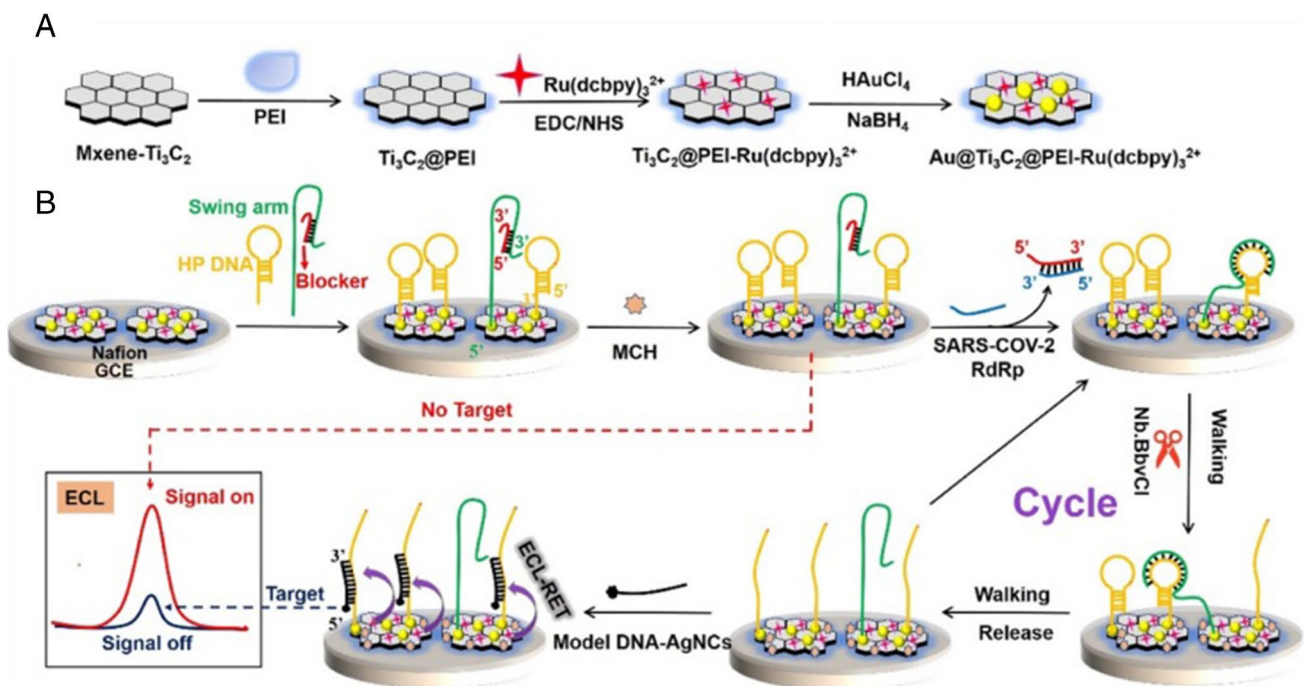


Fig. 8 Schematic illustration of **A** preparation of Au@Ti₃C₂@PEI-Ru(dcbpy)₃²⁺ nanocomposite; **B** Au@Ti₃C₂@PEI-Ru(dcbpy)₃²⁺ ECL biosensor for detection of SARS-CoV-2 RdRp gene combined

unipedal DNA walker amplification strategy [80]; reprinted by permission from ACS Publisher

sample. The value estimated for the LOD was found to be 514 aM.

LSPR colorimetric sensing methods

Colorimetric biosensors based on the localized surface plasmon resonance (LSPR) of AuNPs have shown enhanced capabilities for the determination of biological targets, such as viruses [84]. The remarkable advantages of AuNP-based LSPR colorimetric biosensors, such as multiplexing capability, high sensitivity, and ability to miniature, make them interesting candidates for the PoC diagnosis [85]. Qiu et al. [83] developed a dual-purpose plasmonic genosensor combined with plasmon photothermal (PPT) and LSPR transducer for the diagnosis of COVID-19. As seen in Fig. 9, this genosensor was based on the hybridization of gold nanoisland (AuNI)-functionalized cDNA bioreceptors with RdRP genes. To increase sensor performance, plasmonic resonance frequency was irradiated on the AuNIs to generate thermoplasmonic heat on the same chip. The localized PPT heat increased the in situ hybridization temperature, which promotes the ability to accurately detect two similar gene sequences. In fact, increasing in situ PPT on the AuNI chips significantly increased the specificity of nucleic acid detection by dramatically improving hybridization kinetics. As the designed LSPR genosensor allowed precise detection of SARS-CoV-2 RdRP in a multigene mixture and also showed a high sensitivity toward the target sequences with a LOD of 0.22 pM.

In another attempt, Kim et al. [86] proposed a sensing strategy based on the dsDNA-covered AuNPs for the determination of the E gene and ORF1a. As seen in Fig. 10, the target gene-oligo probe duplex formed a disulfide-induced self-assembled complex that protected AuNPs from

salt-induced aggregation and transition of optical properties. However, salt-induced aggregation of AuNPs was observed in the absence of target genes. This biosensor could determine target genes using a LSPR shift and color changes of AuNPs in the UV-Vis wavelength range and discriminate down to 1 pmol μL^{-1} of 30 bp MERS-CoV.

Huang and co-workers [87] reported the determination of SARS-CoV-2 pseudoviruses using the plasmonic sensor based on the Au-TiO₂-Au nanocup array chip within 15 min. They detected as few as 30 virus particles in one step and quantified the virus concentration linearly in the range of 103 to 106 vp mL⁻¹.

SERS-based sensing methods

For sensitive determination of biological analytes, a number of new sensing strategies have been developed using the surface-enhanced Raman scattering (SERS). This technique can overcome the inherent weakness of Raman spectroscopy. The SERS as a field-deployable, label-free, and non-destructive technique is able to detect biomarkers for early diagnosis of diseases using the Raman signals amplified by AuNPs [88]. So, AuNPs have been widely used as the effective SERS substrates in the configuration of biosensors [89]. The SERS nanotags are fabricated by binding strong Raman active molecules to AuNPs [90]. These nanotags are simply attached with the various bioreceptors for the selective targeting of biomarkers [90].

In this regard, Gao et al. [91] proposed a three-modal genosensor based on the colorimetric/SERS/fluorescence for the SARS-CoV-2 RNA detection. Based on the aggregation of AuNPs, the presented biosensor achieved a LOD of femtomole in all modes, which is 160 fM in absorbance mode, 259 fM in fluorescence mode, and 395 fM in SERS mode.

Fig. 9 Schematic representation for the dual-functional PPT enhanced LSPR biosensing strategy for detection of SARS-CoV-2 RdRP gene [83]; reprinted by permission from ACS Publisher

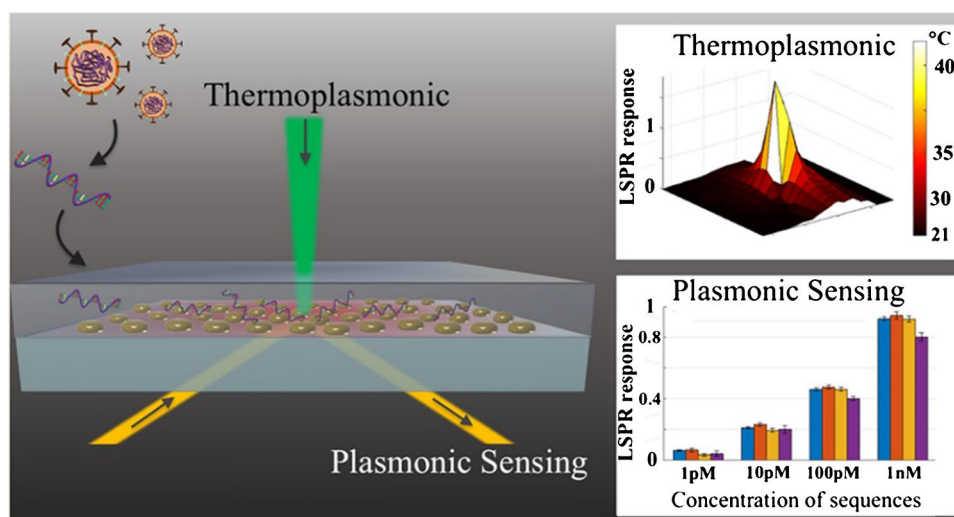
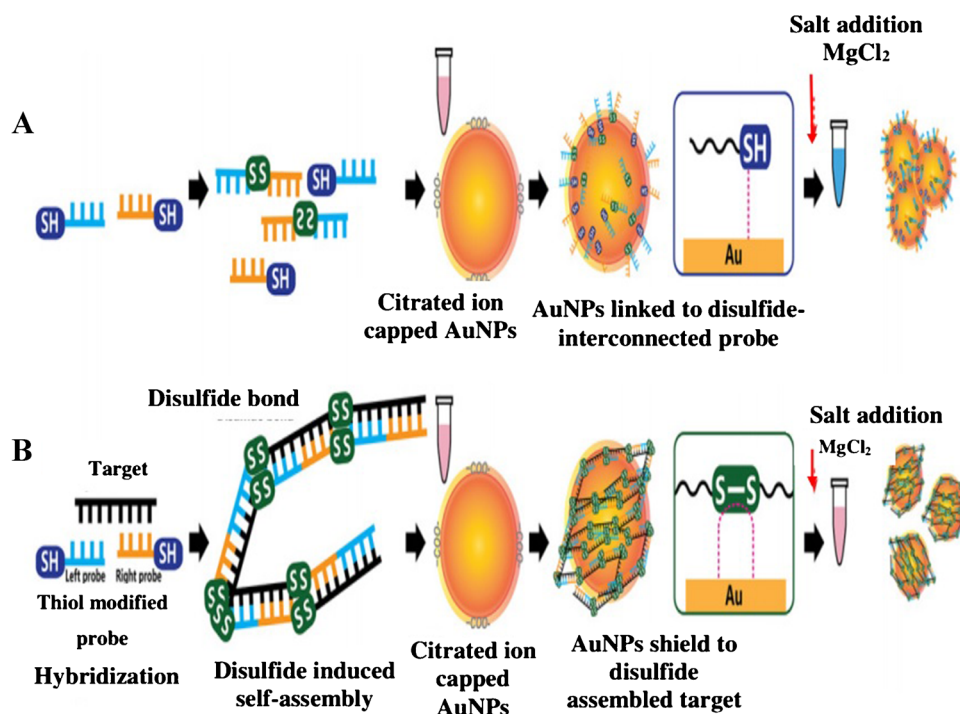


Fig. 10 Schematic illustration of a sensing strategy based on the dsDNA-covered AuNPs for the determination of E gene and ORF1a; **A** salt-induced aggregation of AuNPs in the absence of target genes and **B** the target gene-oligo probe duplex formed a disulfide-induced self-assembled complex that protected AuNPs from salt-induced aggregation [86]; reprinted by permission from ACS Publisher



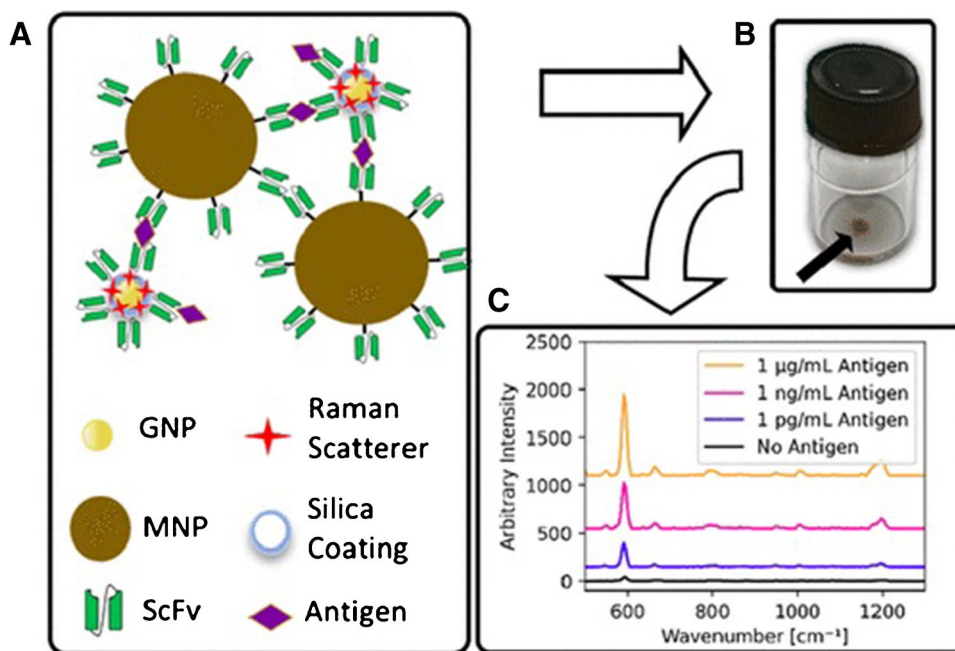
Wu and co-workers [92] suggested a SERS-PCR strategy for the detection of SARS-CoV-2 genes (E and RdRP genes) using AuNP-internalized Au nanodimple substrates (AuNDS). According to the obtained results from RT-PCR, SERS-PCR, and AuNDS-based SERS-PCR, the detectable concentrations of genes were found to be 3.36×10^{12} , 3.28×10^9 , and 2.56×10^7 copies μL^{-1} , respectively. As seen, the AuNDS-based SERS-PCR is a preferred method compared to the RT-PCR and SERS-PCR. In addition, AuNDS-based SERS-PCR reduced detection time by decreasing the number of thermocycling steps required for DNA amplification. Bistaffa et al. [93] designed an immunosensing strategy based on the SERS of methylene blue (MB) adsorbed onto AuNPs and coated with a silica shell. This SERS immunoassay detected SARS-CoV-2 S protein with a LOD of 0.046 ng mL^{-1} (0.60 pM). Cha et al. [94] proposed a magnetically assisted immunosensor consisting of the reporter antibody, malachite green isothiocyanate conjugated hollow AuNPs, and antibody-conjugated magnetic beads for the SARS-CoV-2 determination. In this study, malachite green was utilized as a popular Raman dye that generates a distinct spectrum. With the introduction of antigen, the AuNPs were assembled with the magnetic beads through immunoreactions between the antibody pairs and the CoVs in the sample. Thus, the strong SERS signals of malachite green were observed in the presence of SARS-CoV-2 antigen due to the formation of AuNPs carrying malachite green. The peak intensity increased linearly from 10 fg mL^{-1} to 100 pg mL^{-1} with a LOD of 2.56 fg mL^{-1} . Chen and co-workers [95] designed a SERS aptasensor to quantify the

SARS-CoV-2 S protein. They used an anti-S protein aptamer and self-grown Au nanopopcorns. The binding between the aptamer separated from the Au nanopopcorns and S antigen led to a change in the SERS peak intensity. The presented protocol enabled S protein determination with a LOD of 10 PFU mL^{-1} . Antoine et al. [96] reported a magnetic SERS immunosensor for the detection of SARS-CoV-2 S antigen (Fig. 11). The single-chain Fv (scFv) recombinant Ab fragments were conjugated to magnetic beads and AuNPs (with a Raman scatterer) and form immunocomplexes in the presence of S protein. Using this SERS immunodetection, a LOD of 257 fg mL^{-1} in the viral medium was obtained. In another attempt, Pramanik and co-workers [65] designed a SERS immunosensor based on the 4-aminothiophenol and antibody-functionalized AuNPs for the S antigen determination. In this study, 4-aminothiophenol was used as a reporter molecule. The antigen-antibody reaction led to the aggregation of AuNPs and the formation of hot spots. The hot spot formation has a significant effect on the dramatic enhancement of SERS signals. So, this strategy allowed the sensitive quantification of SARS-CoV-2 S protein with LOD of $\sim 4 \text{ pg mL}^{-1}$.

Fluorescence-based sensing methods

Huang and co-workers [97] developed a localized surface plasmon coupled fluorescence (LSPCF) fiber-optic biosensor for the determination of SARS-CoV N protein. They used a combination of sandwich immunosensing with the

Fig. 11 A Schematic illustration of SERS-immunosensing assay based on the scFvs conjugated to magnetic beads and AuNPs (with a Raman scatterer), B collected magnetic beads in the presence of an external magnet, and C SERS spectrum [96]; reprinted by permission from ACS Publisher



LSP technique. The fluorescence probe was composed of fluorophores (DyLight™) which were labeled with the secondary antibodies connecting to AuNP conjugate protein A (Au-PA). In this work, a linear relationship was obtained between the fluorescence signal and the N protein concentration from 0.1 pg mL^{-1} to 1 ng mL^{-1} in the buffer solution and diluted serum. The proposed biosensor made it possible to determine the low serum concentration ($\sim 1 \text{ pg mL}^{-1}$) of SARS-CoV-1 N protein.

Other sensing methods

The dynamic light scattering (DLS) technique can be applied for the determination of the SARS-CoV-2 antigen. da Silva and co-workers [98] utilized this method using the antibody-functionalized AuNP bioconjugate. The specific binding of the S antigen to the antibody resulted in an increase of bioconjugate size, with a LOD $5.29 \times 10^3 \text{ TCID}_{50} \text{ mL}^{-1}$ (tissue culture infectious dose). In another attempt, Xu and co-workers [99] reported a single-particle inductively coupled plasma mass spectrometry (SP-ICP-MS)-based biosensor for the SARS-CoV-2 detection. The single-particle (SP)-ICP-MS is a special ICP-MS detection strategy. In this method, short transient signals emanating from single nanoparticles (usually AuNPs) are recorded in a measurement of the dissolved time by reducing the residence time in the millisecond time regime [100]. Based on these advantages, a SP-ICP-MS technique was utilized for the RNA detection using the AuNPs. In the presence of SARS-CoV-2 RNA, the AuNPs aggregated to form larger particles, which

increased the pulse signal intensity and decreased the pulse signal frequency of nanoparticles. This method showed a good potential for detecting nucleic acid in the linear range of $5\text{--}1000 \text{ pmol L}^{-1}$.

AuNP-based sensing methods for other coronaviruses

Human coronaviruses are classified into two general types, low pathogenic and highly pathogenic. Unlike SARS-CoV-1, MERS-CoV, and SARS-CoV-2, low pathogenic human CoVs (229E, OC43, NL63, and HKU1) cause mild to moderate upper respiratory illness, which accounts for 15 to 30% of colds in humans [101]. Due to their lower pathogenicity, very few studies have been done on the detection strategies of these coronaviruses. In this regard, there is only one research for the determination of OC43 N protein. Layqah and Eissa [40] fabricated a voltammetric immunosensor for the OC43 N detection using an array of AuNP-modified carbon electrodes. A good linear relationship between the electrode responses and target concentrations was observed from 0.01 to $10,000 \text{ ng mL}^{-1}$. This sensing protocol was performed with a LOD of 0.4 pg mL^{-1} within 20 min.

Conclusion

The incorporation of AuNPs into the biosensing technology offers reliable and sensitive detection of coronaviruses. AuNPs have a profound impact on the biosensing strategies

due to their unique characteristics, such as easy preparation, simple surface modification, high conductivity, and electrocatalytic ability. Additionally, the surface plasmons of AuNPs exhibit unique features underlying their strong absorption. This manuscript provides an up-to-date overview to discuss the current AuNP-based sensing strategies for the detection of highly and lowly pathogenic human coronaviruses. The described protocols were compared in terms of detection mechanisms, bioreceptors, surface modifications, and figures of merit. Based on these studies, we have several suggestions for increasing the efficiency of biosensors: (I) integration of biosensors with microfluidic chips to achieve continual, noninvasive, and in situ quantification of biomarkers on organ-on-a-chip platforms; (II) portable systems for indoor and outdoor applications; (III) multiplexed determination that reduces false-negative possibility; and (IV) in vivo biosensors for continuous and long-term monitoring of analytes in the biological samples. The use of at least two targets for the SARS-CoV-2 determination provides higher accuracy and reliability.

Declarations

Conflict of interest The authors declare no competing interests.

References

- Bhalla N, Pan Y, Yang Z, Payam AF. Opportunities and challenges for biosensors and nanoscale analytical tools for pandemics: COVID-19. *ACS Nano*. 2020;14:7783–807.
- Randall RE, Griffin DE. Within host RNA virus persistence: mechanisms and consequences. *Curr Opin Viral*. 2017;23:35–42.
- Wang C, Wang C, Qiu J, Gao J, Liu H, Zhang Y, et al. Ultrasensitive, high-throughput, and rapid simultaneous detection of SARS-CoV-2 antigens and IgG/IgM antibodies within 10 min through an immunoassay biochip. *Microchim Acta*. 2021;188:262.
- Ahmed W, Simpson SL, Bertsch PM, Bibby K, Bivins A, Blackall LL, et al. Minimizing errors in RT-PCR detection and quantification of SARS-CoV-2 RNA for wastewater surveillance. *Sci Total Environ*. 2022;805:149877.
- Farzin L, Sadjadi S, Sheini A, Mohaghehpour E. A nanoscale genosensor for early detection of COVID-19 by voltammetric determination of RNA-dependent RNA polymerase (RdRP) sequence of SARS-CoV-2 virus. *Microchim Acta*. 2021;188:121.
- Alhadrami HA, Hassan AM, Chinnappan R, Al-handrami H, Abdulaal WH, Azhar EI, et al. Peptide substrate screening for the diagnosis of SARS-CoV-2 using fluorescence resonance energy transfer (FRET) assay. *Microchim Acta*. 2021;188:137.
- Shamsipur M, Emami M, Farzin L, Saber R. A sandwich-type electrochemical immunosensor based on in situ silver deposition for determination of serum level of HER2 in breast cancer patients. *Biosens Bioelectron*. 2018;103:54–61.
- Saha K, Agasti SS, Kim C, Li X, Rotello VM. Gold nanoparticles in chemical and biological sensing. *Chem Rev*. 2012;112:2739–79.
- Huang X, El-sayed MA. Gold nanoparticles: optical properties and implementations in cancer diagnosis and photothermal therapy. *J Adv Res*. 2010;1:13–28.
- Mohapatra S, Mishra YK, Avasth DK, Kabiraj D, Ghatak J, Varma S. Synthesis of gold-silicon core-shell nanoparticles with tunable localized surface plasmon resonance. *Appl Phys Lett*. 2008;92:103105.
- Li S, Zhang T, Zhu Z, Gao N, Xu QH. Lighting up the gold nanoparticles quenched fluorescence by silver nanoparticles: a separation distance study. *RSC Adv*. 2016;6:58566–72.
- Asnaashari M, Kenari RE, Farahmandfar R, Taghdisi SM, Abnous K. Fluorescence quenching biosensor for acrylamide detection in food products based on double-stranded DNA and gold nanoparticles. *Sensors Actuators B Chem*. 2018;265:339–45.
- Wang W, Kong T, Zhang D, Zhang J, Cheng G. Label-free MicroRNA detection based on fluorescence quenching of gold nanoparticles with a competitive hybridization. *Anal Chem*. 2015;87:10822–9.
- Lv X, Zhang Y, Liu G, Du L, Wang S. Aptamer-based fluorescent detection of ochratoxin A by quenching of gold nanoparticles. *RSC Adv*. 2017;7:16290–4.
- Shamsipur M, Farzin L, Tabrizi MA. Ultrasensitive aptamer-based on-off assay for lysozyme using a glassy carbon electrode modified with gold nanoparticles and electrochemically reduced graphene oxide. *Microchim Acta*. 2016;183:2733–43.
- Roushani M, Shahdost-Fard F. Fabrication of an electrochemical nanoaptasensor based on AuNPs for ultrasensitive determination of cocaine in serum sample. *Mater Sci Eng C Mater Biol Appl*. 2016;61:599–607.
- Young SL, Kellon JE, Hutchison JE. Small gold nanoparticles interfaced to electrodes through molecular linkers: a platform to enhance electron transfer and increase electrochemically active surface area. *J Am Chem Soc*. 2016;138:13975–84.
- Guo C, Wang J, Chen X, Li Y, Wu L, Zhang J, et al. Construction of a biosensor based on a combination of cytochrome *c*, graphene, and gold nanoparticles. *Sensors*. 2019;19:40.
- Yu A, Liang Z, Cho J, Caruso F. Nanostructured electrochemical sensor based on dense gold nanoparticle films. *Nano Lett*. 2003;3:1203–7.
- Zhu W, Michalsky R, Metin O, Lv H, Guo S, Wright CJ, et al. Monodisperse Au nanoparticles for selective electrocatalytic reduction of CO₂ to CO. *J Am Chem Soc*. 2013;135:16833–6.
- Bharath G, Naldoni A, Ramsait KH, Abdel-Wahab A, Madhu R, Alsharaeh E, et al. Enhanced electrocatalytic activity of gold nanoparticles on hydroxyapatite nanorods for sensitive hydrazine sensors. *J Mater Chem A*. 2016;4:6385–94.
- Zhang J, Lahtinen RM, Kontturi K, Unwin PR, Schiffrin DJ. Electron transfer reactions at gold nanoparticles. *Chem Commun*. 2001;18:1818–9.
- Mollarasouli F, Zare-Shehneh N, Ghaedi M. A review on corona virus disease 2019 (COVID-19): current progress, clinical features and bioanalytical diagnostic methods. *Microchim Acta*. 2022;189:103.
- Bu J, Deng Z, Liu H, Li J, Wang D, Yang Y, et al. Current methods and prospects of coronavirus detection. *Talanta*. 2021;225:121977.
- Drobysch M, Ramanaviciene A, Viter R, Chen CF, Samukaite-Bubniene U, Ratautaite V, et al. Biosensors for the determination of SARS-CoV-2 virus and diagnosis of COVID-19 infection. *Int J Mol Sci*. 2022;23:666.
- Hamidi-Asl E, Heidari-Khoshkelat L, Raouf JB, Richard TP, Farhad S, Ghani M. A review on the recent achievements on coronaviruses recognition using electrochemical detection methods. *Microchem Acta*. 2022;178:107322.

27. Dhar BC. Diagnostic assay and technology advancement for detecting SARS-CoV-2 infections causing the COVID-19 pandemic. *Anal Bioanal Chem.* 2022;414:2903–34.
28. Aquino A, Paschoalin VMF, Tessaro LLG, Raymundo-Pereira PA, Conte-Junior CA. Updating the use of nano-biosensors as promising devices for the diagnosis of coronavirus family members: a systematic review. *J Pharm Biomed Anal.* 2022;211:114608.
29. Mobed A, Shafiq ES. Biosensors promising bio-device for pandemic screening “COVID-19”. *Microchem J.* 2021;164:106094.
30. Miripour ZS, Sarrami-Forooshani R, Sanati H, Makarem J, Taheri MS, Shojaeian F, et al. Real-time diagnosis of reactive oxygen species (ROS) in fresh sputum by electrochemical tracing; correlation between COVID-19 and viral-induced ROS in lung/respiratory epithelium during this pandemic. *Biosens Bioelectron.* 2020;165:112435.
31. V'kovski P, Kratzel A, Steiner S, Stalder H, Thiel V. Coronavirus biology and replication: implications for SARS-CoV-2. *Nat Rev Microbiol.* 2021;19:155–70.
32. Etienne EE, Nunna BB, Talukder N, Wang Y, Lee ES. COVID-19 biomarkers and advanced sensing technologies for point-of-care (POC) diagnosis. *Bioengineering.* 2021;8:98.
33. Rat P, Olivier E, Dutot M. SARS-CoV-2 vs. SARS-CoV-1 management: antibiotics and inflammasome modulators potential. *Eur Rev Med Pharmacol Sci.* 2020;24:7880–5.
34. Caldaria A, Conforti C, Meo ND, Dianzani C, Jafferany M, Lotti T, et al. COVID-19 and SARS: differences and similarities. *Dermatol Ther.* 2020;33:e13395.
35. Harrison AG, Lin T, Wang P. Mechanisms of SARS-CoV-2 transmission and pathogenesis. *Trends Immunol.* 2020;41:1100–15.
36. Zhu Z, Lian X, Su X, Wu W, Marrao GA, Zeng Y. From SARS and MERS to COVID-19: a brief summary and comparison of severe acute respiratory infections caused by three highly pathogenic human coronaviruses. *Respir Res.* 2020;21:224.
37. Chong ZX, Liew WPP, Ong HK, Yong CY, Shit CS, Ho WY, et al. Current diagnostic approaches to detect two important beta-coronaviruses: Middle East respiratory syndrome coronavirus (MERS-CoV) and severe acute respiratory syndrome coronavirus 2 (SARS-CoV-2). *Pathol Res Pract.* 2021;225:153565.
38. Besharati M, Tabrizi MA, Molaabasi F, Saber R, Shamsipur M, Hamed J, et al. Novel enzyme-based electrochemical and colorimetric biosensors for tetracycline monitoring in milk. *Biotechnol Appl Biochem.* 2022;69:41–50.
39. Farzin MA, Abdoos H. A critical review on quantum dots: from synthesis toward applications in electrochemical biosensors for determination of disease-related biomolecules. *Talanta.* 2021;224:121828.
40. Layqah LA, Eissa S. An electrochemical immunosensor for the corona virus associated with the Middle East respiratory syndrome using an array of gold nanoparticle-modified carbon electrodes. *Microchim Acta.* 2019;186:224.
41. Mahari S, Roberts A, Shahdeo D, Gandhi S. eCovSens-ultrasensitive novel in-house built printed circuit board based electrochemical device for rapid detection of Covid-19 antigen, a spike protein domain 1 of SARS-CoV-2. *BioRxiv.* 2020.
42. Alafeef M, Dighe K, Moitra P, Pan D. Rapid, ultrasensitive, and quantitative detection of SARS-CoV-2 using antisense oligonucleotides directed electrochemical biosensor chip. *ACS Nano.* 2020;14:17028–45.
43. Karakus E, Erdemir E, Demirbilek N, Liv L. Colorimetric and electrochemical detection of SARS-CoV-2 spike antigen with a gold nanoparticle-based biosensor. *Anal Chim Acta.* 2021;1182:338939.
44. El-Said WA, Al-Bogami AS, Alshitari W, El-Hady DA, Saleh TS, El-Mokhtar MA, et al. Electrochemical microbiosensor for detecting COVID-19 in a patient sample based on gold micro-cuboids pattern. *Biochip J.* 2021;15:287–95.
45. Karaman C, Yola BB, Karaman O, Atar N, Polat I, Yola ML. Sensitive sandwich-type electrochemical SARS-CoV-2 nucleocapsid protein immunosensor. *Microchim Acta.* 2021;188:425.
46. Roberts A, Mahari S, Shahdeo D, Gandhi S. Label-free detection of SARS-CoV-2 Spike S1 antigen triggered by electroactive gold nanoparticles on antibody coated fluorine-doped tin oxide (FTO) electrode. *Anal Chim Acta.* 2021;1188:339207.
47. Hashemi SA, Bahrani S, Mousavi SM, Omidifar N, Behbahan NGG, Arjmand M, et al. Antibody mounting capability of 1D/2D carbonaceous nanomaterials toward rapid-specific detection of SARS-CoV-2. *Talanta.* 2022;239:123113.
48. Tabeizi MA, Fernández-Blázquez JP, Medina DM, Acedo P. An ultrasensitive molecularly imprinted polymer-based electrochemical sensor for the determination of SARS-CoV-2-RBD by using macroporous gold screen-printed electrode. *Biosens Bioelectron.* 2022;196:113729.
49. Ramanathan S, Gopinath SCB, Ismail ZH, Md Arshad MK, Poopalan P. Aptasensing nucleocapsid protein on nanodiamond assembled gold interdigitated electrodes for impedimetric SARS-CoV-2 infectious disease assessment. *Biosens Bioelectron.* 2022;197:113735.
50. Tian J, Liang Z, Hu O, He Q, Sun D, Chen Z. An electrochemical dual-aptamer biosensor based on metal-organic frameworks MIL-53 decorated with Au@Pt nanoparticles and enzymes for detection of COVID-19 nucleocapsid protein. *Electrochim Acta.* 2021;387:138553.
51. Zhao H, Liu F, Xie W, Zhou TC, Yang JO, Jin L, et al. Ultrasensitive supersandwich-type electrochemical sensor for SARS-CoV-2 from the infected COVID-19 patients using a smartphone. *Sensors Actuators B Chem.* 2021;327:128899.
52. Zamora-Mendoza BN, de León-Martínez LD, Rodríguez-Agüilar M, Mizaikoff B, Flores-Ramírez R. Chemometric analysis of the global pattern of volatile organic compounds in the exhaled breath of patients with COVID-19, post-COVID and healthy subjects. Proof of concept for post-COVID assessment. *Talanta.* 2022;236:122832.
53. Tripathy S, Singh SG. Label-free electrochemical detection of DNA hybridization: a method for COVID-19 diagnosis. *Trans Indian Nat Acad Eng.* 2020;5:205–9.
54. Munoz J, Pumera M. 3D-printed COVID-19 immunosensors with electronic readout. *Chem Eng J.* 2021;425:131433.
55. Heo W, Lee K, Park S, Hyun KA, Jung HI. Electrochemical biosensor for nucleic acid amplification-free and sensitive detection of severe acute respiratory syndrome coronavirus 2 (SARS-CoV-2) RNA via CRISPR/Cas13a trans-cleavage reaction. *Biosens Bioelectron.* 2022;201:113960.
56. Mehmandoust M, Gumus ZP, Soylyak M, Erk N. Electrochemical immunosensor for rapid and highly sensitive detection of SARS-CoV-2 antigen in the nasal sample. *Talanta.* 2022;240:123211.
57. Brazaco LC, Imamura AH, Gomes NO, Almeida MB, Scheidt DT, Raymundo-Pereira PA, et al. Electrochemical immunosensors using electrodeposited gold nanostructures for detecting the S proteins from SARS-CoV and SARS-CoV-2. *Anal Bioanal Chem.* 2022;592:1.
58. Avelino KYPS, dos Santos GS, Frias IAM, Silva-Junior AG, Pereira MC, Pitta MGR, et al. Nanostructured sensor platform based on organic polymer conjugated to metallic nanoparticle for the impedimetric detection of SARS-CoV-2 at various stages of viral infection. *J Pharm Biomed Anal.* 2021;206:114392.
59. Nascimento ED, Fonseca WT, de Oliveira TR, de Correia CRSTB, Faca VM, de Moraes BP, et al. COVID-19 diagnosis by SARS-CoV-2 Spike protein detection in saliva using an

- ultrasensitive magneto-assay based on disposable electrochemical sensor. *Sensors Actuators B Chem.* 2022;353:131128.
60. Farzin MA, Abdoos H, Saber S. Graphite nanocrystals coated paper-based electrode for detection of SARS-Cov-2 gene using DNA-functionalized Au@carbon dot core-shell nanoparticles. *Microchem J.* 2022;179:107585.
 61. Bakhtiari SA, Abdoos H, Karimzadeh F. Green synthesis of ZnO@ZnS core-shell nanoparticles for detection of lead and iron ions in aqueous solutions by colorimetric paper sensors. *Chem Papers.* 2022;76:99–109.
 62. Rodríguez-Díaz C, Lafuente-Gómez N, Coutinho C, Pardo D, Alarcón-Iniesta H, López-Valls M, et al. Development of colorimetric sensors based on gold nanoparticles for SARS-CoV-2 RdRp, E and S genes detection. *Talanta.* 2022;243:123393.
 63. Kumar V, Mishra S, Sharma R, Agarwal J, Ghoshal U, Khanna T, et al. Development of RNA-based assay for rapid detection of SARS-CoV-2 in clinical samples. *bioRxiv.* 2022.
 64. Alafeef M, Moitra P, Dighe K, Pan D. RNA-extraction-free nano-amplified colorimetric test for point-of-care clinical diagnosis of COVID-19. *Nat Protoc.* 2021;16:3141–62.
 65. Pramanik A, Gao Y, Patibandla S, Mitra D, McCandless MG, Fassero LA, et al. The rapid diagnosis and effective inhibition of coronavirus using spike antibody attached gold nanoparticles. *Nanoscale Adv.* 2021;3:1588–96.
 66. Ventura BD, Cennamo M, Minopoli A, Campanile R, Censi SB, Terracciano D, et al. Colorimetric test for fast detection of SARS-CoV-2 in nasal and throat swabs. *ACS Sensors.* 2020;5:3043–8.
 67. Moitra P, Alafeef M, Dighe K, Frieman MB, Pan D. Selective naked-eye detection of SARS-CoV-2 mediated by N gene targeted antisense oligonucleotide capped plasmonic nanoparticles. *ACS Nano.* 2020;14:7617–27.
 68. Aithal S, Mishriki S, Gupta R, Sahu RP, Botos G, Tanvir S, et al. SARS-CoV-2 detection with aptamer-functionalized gold nanoparticles. *Talanta.* 2022;236:122841.
 69. Tabrizi AM, Shamsipur M, Saber R, Sarkar S, Ebrahimi V. A high sensitive visible light-driven photoelectrochemical aptasensor for shrimp allergen tropomyosin detection using graphitic carbon nitride-TiO₂ nanocomposite. *Biosens Bioelectron.* 2017;98:113–8.
 70. Behrouzi K, Lin L. Gold nanoparticle based plasmonic sensing for the detection of SARS-CoV-2 nucleocapsid proteins. *Biosens Bioelectron.* 2022;195:113669.
 71. Sohail M, Xie S, Zhang X, Li B. Methodologies in visualizing the activation of CRISPR/Cas: the last mile in developing CRISPR-Based diagnostics and biosensing—a review. *Anal Chim Acta.* 2022;1205:339541.
 72. Luo X, Xue Y, Ju E, Tao Y, Li M, Zhou L, et al. Digital CRISPR/Cas12b-based platform enabled absolute quantification of viral RNA. *Anal Chim Acta.* 2022;1192:339336.
 73. Zhou T, Huang R, Huang M, Shen J, Shan Y, Xing D. CRISPR/Cas13a powered portable electrochemiluminescence chip for ultrasensitive and specific MiRNA detection. *Adv Sci.* 2020;7:1903661.
 74. Zhang K, Fan Z, Yao B, Ding Y, Zhao J, Xie M, et al. Exploring the trans-cleavage activity of CRISPR-Cas12a for the development of a Mxene based electrochemiluminescence biosensor for the detection of Siglec-5. *Biosens Bioelectron.* 2021;178:113019.
 75. Cao Y, Wu J, Pang B, Zhang H, Le XC. CRISPR/Cas12a-mediated gold nanoparticle aggregation for colorimetric detection of SARS-CoV-2. *Chem Commun.* 2021;57:6871–4.
 76. Ma L, Yin L, Li X, Chen S, Peng L, Liu G, et al. A smartphone-based visual biosensor for CRISPR-Cas powered SARS-CoV-2 diagnostics. *Biosens Bioelectron.* 2022;195:113646.
 77. Jiang Y, Hu M, Liu AA, Lin Y, Liu L, Yu B, et al. Detection of SARS-CoV-2 by CRISPR/Cas12a-enhanced colorimetry. *ACS Sens.* 2021;6:1086–93.
 78. Zhang K, Fan Z, Yao B, Zhang T, Ding Y, Zhu S, et al. Entropy-driven electrochemiluminescence ultra-sensitive detection strategy of NF-κB p50 as the regulator of cytokine storm. *Biosens Bioelectron.* 2021;176:112942.
 79. Zhang K, Fan Z, Huang Y, Ding Y, Xie M. A strategy combining 3D-DNA Walker and CRISPR-Cas12a trans-cleavage activity applied to MXene based electrochemiluminescent sensor for SARS-CoV-2 RdRp gene detection. *Talanta.* 2022;236:122868.
 80. Yao B, Zhang J, Fan Z, Ding Y, Zhou B, Yang R, et al. Rational engineering of the DNA walker amplification strategy by using a Au@Ti₃C₂@PEI-Ru(dcbpy)₃²⁺ nanocomposite biosensor for detection of the SARS-CoV-2 RdRp gene. *ACS Appl Mater Interfaces.* 2021;13:19816–24.
 81. Zhang K, Fan Z, Huang Y, Ding Y, Xie M, Wang M. Hybridization chain reaction circuit-based electrochemiluminescent biosensor for SARS-cov-2 RdRp gene assay. *Talanta.* 2022;240:123207.
 82. Gutiérrez-Gálvez L, del Cano R, Menéndez-Luque I, García-Nieto D, Rodríguez-Peña M, Luna M, et al. Electrochemiluminescent nanostructured DNA biosensor for SARS-CoV-2 detection. *Talanta.* 2022;240:123203.
 83. Qiu G, Gai Z, Tao Y, Schmitt J, Kullak-Ublick GA, Wang J. Dual-functional plasmonic photothermal biosensors for highly accurate severe acute respiratory syndrome coronavirus 2 detection. *ACS Nano.* 2020;14:5268–77.
 84. Oh SY, Heo NS, Bajpai VK, Jang SC, Ok G, Cho Y, et al. Development of a cuvette-based LSPR sensor chip using a plasmonically active transparent strip. *Front Bioeng Biotechnol.* 2019;7:299.
 85. Lopez GA, Estevez MC, Soler M, Lechuga LM. Recent advances in nanoplasmonic biosensors: applications and lab-on-a-chip integration. *Nanophotonics.* 2016;6:123–36.
 86. Kim H, Park M, Hwang J, Kim JH, Chung DR, Lee K, et al. Development of label-free colorimetric assay for MERS-CoV using gold nanoparticles. *ACS Sens.* 2019;4:1306–12.
 87. Huang L, Ding L, Zhou J, Chen S, Chen F, Zhao C, et al. One-step rapid quantification of SARS-CoV-2 virus particles via low-cost nanoplasmonic sensors in generic microplate reader and point-of-care device. *bioRxiv.* 2020.
 88. Azimi S, Docoslis A. Recent advances in the use of surface-enhanced Raman scattering for illicit drug detection. *Sensors* 2022;22:3877.
 89. Arbutz A, Sultangazyev A, Rapikov A, Kunushpayeva Z, Bukasov R. How gap distance between gold nanoparticles in dimers and trimers on metallic and non-metallic SERS substrates can impact signal enhancement. *Nanoscale Adv.* 2022;4:268–80.
 90. Dinis US, Balasundaram G, Chang YT, Olivo M. Actively targeted *in vivo* multiplex detection of intrinsic cancer biomarkers using biocompatible SERS nanotags. *Sci Rep.* 2014;4:4075.
 91. Gao Y, Han Y, Wang C, Qiang L, Gao J, Wang Y, et al. Rapid and sensitive triple-mode detection of causative SARS-CoV-2 virus specific genes through interaction between genes and nanoparticles. *Anal Chim Acta.* 2021;1154:338330.
 92. Wu Y, Dang H, Park SG, Chen L, Choo J. SERS-PCR assays of SARS-CoV-2 target genes using Au nanoparticles-internalized Au nanodimple substrates. *Biosens Bioelectron.* 2022;197:113736.
 93. Bistaffa MJ, Camacho SA, Pazin WM, Constantino CJL, Oliveira ON Jr, Aoki PHB. Immunoassay platform with surface-enhanced resonance Raman scattering for detecting trace levels of SARS-CoV-2 spike protein. *Talanta.* 2022;244:123381.

94. Cha H, Kim H, Joung Y, Kang H, Moon J, Jang H, et al. Surface-enhanced Raman scattering-based immunoassay for severe acute respiratory syndrome coronavirus 2. *Biosens Bioelectron.* 2022;202:114008.
95. Chen H, Park SG, Choi N, Kwon HJ, Kang T, Lee MK, et al. Sensitive detection of SARS-CoV-2 using a SERS-based aptasensor. *ACS Sens.* 2021;6:2378–85.
96. Antoine D, Mohammadi M, Vitt M, Dickie JM, Jyoti SS, Tibury MA, et al. Rapid, point-of-care scFv-SERS assay for femtogram level detection of SARS-CoV-2. *ACS Sens.* 2022;7:866–73.
97. Huang JC, Chang YF, Chen KH, Su LC, Lee CW, Chen CC, et al. Detection of severe acute respiratory syndrome (SARS) coronavirus nucleocapsid protein in human serum using a localized surface plasmon coupled fluorescence fiber-optic biosensor. *Biosens Bioelectron.* 2009;25:320–5.
98. da Silva PB, da Silva JR, Rodrigues MC, Vieira JA, de Andrade IA, Nagata T, et al. Detection of SARS-CoV-2 virus via dynamic light scattering using antibody-gold nanoparticle bioconjugates against viral spike protein. *Talanta.* 2022;243:123355.
99. Xu Y, Chen B, He M, Hu B. A homogeneous nucleic acid assay for simultaneous detection of SARS-CoV-2 and influenza A (H3N2) by single-particle inductively coupled plasma mass spectrometry. *Anal Chim Acta.* 2021;1186:339134.
100. Streng I, Engelhard C. Capabilities of fast data acquisition with microsecond time resolution in inductively coupled plasma mass spectrometry and identification of signal artifacts from millisecond dwell times during detection of single gold nanoparticles. *J Anal At Spectrom.* 2016;31:135–44.
101. Liu DX, Liang JQ, Fung TS. Human coronavirus-229E, -OC43, -NL63, and -HKU1 (Coronaviridae). *Encyclopedia Virol.* 2021;2021:428–40.

Publisher's note Springer Nature remains neutral with regard to jurisdictional claims in published maps and institutional affiliations.